GeoMCU: Adaptable and Resilient Low-Noise Sensing Platform for Structural Vibrations

Jesse R Codling
codling@umich.edu
University of Michigan
Ann Arbor, Michigan, USA

Yiwen Dong
yiwen@illinois.edu
University of Illinois, Urbana-Champaign
Urbana, Illinois, USA

Carlos Ruiz
carlos@aifi.com
AiFi, Inc
Burlingame, CA, USA

Amelie Bonde
amelie@thesenselab.com
The Sense Lab, Co.
Laurel, MD, USA

Shijia Pan
span24@ucmerced.edu
University of California, Merced
Merced, CA, USA

Hae Young Noh
noh@stanford.edu
Stanford University
Stanford, California, USA

Pei Zhang
peizhang@umich.edu
University of Michigan
Ann Arbor, Michigan, USA

Abstract

Accurate and scalable structural vibration sensing is an essential tool for a wide range of applications including human and animal health and safety. We present *GeoMCU*, an open-source, low-noise, sensing platform based around geophones, designed for adaptability and resilience in diverse, real-world environments. *GeoMCU* builds on an iterative, experience-driven development process to yield an adaptable sensor platform which reduces electrical noise interference, allows flexible sensor deployment, and supports high precision and time synchronization where required. Evaluation of the platform shows a 4x reduction in electrical noise and over a 10x increase in mean time between failures compared to prior solutions. Through multiple field deployments—ranging from livestock health monitoring to human heart rate detection and stadium crowd behavior analysis—*GeoMCU* has demonstrated significant advantages in scalability, adaptability, and reliability which present a promising solution for ubiquitous sensing in scientific, industrial, and residential environments.

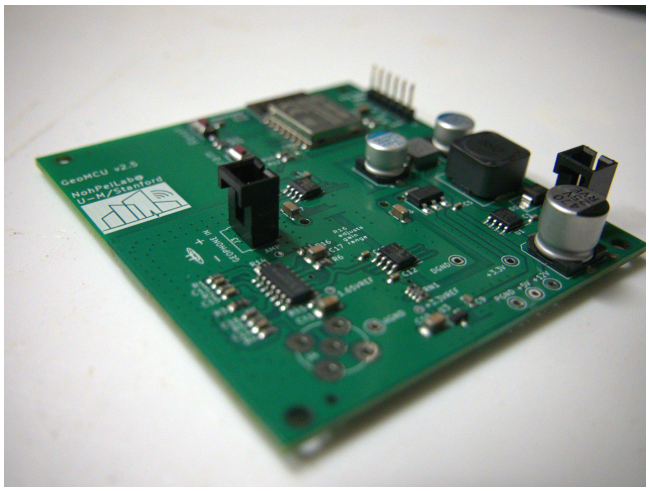

Figure 1: A fully assembled but bare *GeoMCU* sensor board.

CCS Concepts

• **Computer systems organization** → **Sensor networks**; **Embedded systems**; *Fault-tolerant network topologies*; • **Human-centered computing** → *Ubiquitous and mobile computing systems and tools*; • **Applied computing** → Consumer health.

Keywords

Vibration Sensing, Geophones, Embedded Systems, Stuctures-as-Sensors

1 Introduction

Structural vibration sensing has been used for a wide variety of sensing applications in recent years. In the macro scale, they have been used for monitoring the health of building and bridge structures to optimize maintenance and safety [1, 59, 60]. Additionally, smaller scale applications have shown their efficacy in monitoring building occupants, including health monitoring [8, 32, 43, 51, 62, 76], person identification [16, 22, 37, 64, 67, 70], and activity recognition [9, 10, 19, 41, 46, 66, 79]. Such works have even been extended to animal monitoring, with similar benefits and sensing applications to humans [5, 11, 15, 17, 31].

While vibration sensing typically relies on commonly available accelerometers, geophone-based systems have shown particular benefit for their scalability and sensitivity to structural variation. In particular, geophones are more sensitive to low-frequency vibrations near the resonant frequency of the structure, which tend to be especially sensitive to small changes in the structure from occupants and structural changes [68, 70]. These lower frequency vibrations also propagate much farther than the higher frequencies typically measured by accelerometers, improving scalability by enabling sparser sensing range [64, 69].

The wide variety of environments in which structural vibrations occur [15, 27, 34, 38, 63] creates a need for adaptability in the sensing platform. For example, in indoor lab environments, the sensor interface can be relatively primitive due to the relatively controlled conditions. However, deployments outdoors or in harsh environments, such as animal pens, require more robust design [5] to withstand the elements and provide reliable data collection. These various environments also require different levels of sensitivity [18], necessitating the ability to adapt the sensor interface to the specific application, which is typically lacking in existing platforms.

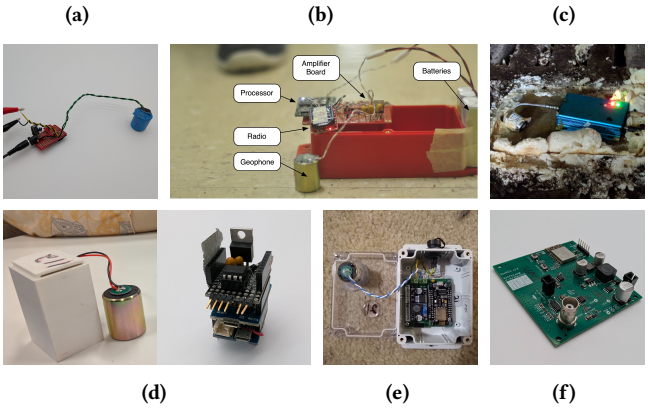

Figure 2: Six geophone interface hardware versions that led up to *GeoMCU*, demonstrating the iterative design evolution.

In this paper, we present *GeoMCU*, an adaptable geophone interface platform for structural vibration sensing developed over several years of iterative design. The balance of this paper will be laid out as follows: Section 2 will detail the iterative design process that led to *GeoMCU*, starting from simple lab prototypes all the way to the most recent versions. Section 3 will present a high-level overview of the *GeoMCU* design, including the design principles derived from the lessons learned in the iterative design process. Section 4 will then detail the uniquely designed components of *GeoMCU* before Section 5 describes *GeoMCU* in a sensor network context, including different configurations in which it can be deployed. In Section 6, we will show some real-world evaluation of *GeoMCU* by presenting some example applications in which it has been used. Section 6 will then evaluate *GeoMCU*'s performance in several real-world applications, demonstrating its adaptability and improvements over previous designs. Finally, we will outline some related works in Section 7 before concluding in Section 8.

2 Iterative Design of Structural Vibration Sensors

GeoMCU builds on many iterations of previous vibration sensing hardware. This includes designs made solely for lab use and those designed for branching out to deployments in remote and harsh environments. With each iteration we have refined our design, learning from the pitfalls and challenges of each.

The earliest hardware versions on which *GeoMCU* is based were hand wired to a prototyping board, as shown in Figure 2a. The only hardware added beyond the geophone itself was a linear regulator, to reduce the noise from typical wall power supplies, and an off-the-shelf operational amplifier board with manual gain adjustment [75]. These wired-only versions were effective for prototyping, but suffered from noise and adaptability problems. Networking was not yet a consideration, nor even remote control or data acquisition since these units were created for lab use with an external data acquisition card. Particularly problematic were the signal losses caused by poor solder joints and high noise from exposed wiring, which necessitated extremely high amplifier gains [62, 70]. These high gains introduced more noise from the amplifier itself, and required delicate modifications to the off-the-shelf hardware to achieve.

To scale beyond lab deployments, we needed something with wireless networking. Some of our first attempts towards this end integrated a low-power Zigbee radio, as shown in Figure 2b. While the Zigbee radio was a good initial choice for prototyping basic connectivity due to its low power requirements and simple interface, the bandwidth requirements for continuously sampling geophone data [71] and the fragmentation of Zigbee hardware led to a non-functional radio data channel. Thus, we had to resort to manually transferring data via SD cards, eliminating the networking capability and hampering the overall deployability of the system. This experience helped us to define the following requirements for our sensor networking setup:

- remote control and configuration capability
- high data bandwidth
- precise time synchronization between multiple nodes sensing the same area

Our next iterations focused on our networking requirements, with particular focus on time synchronization. To this end, we attempted an iteration with a Ultra-Wideband (UWB) radio [57] but were only able to use it for time synchronization due to the bandwidth requirements. While extremely precise, this synchronization was overkill for the geophones, whose sensitivity range tops out around 240 Hz [64]. Building from these challenges with wireless sensors, we switched focus to creating a fairly robust version using wired ethernet. This version resolved the bandwidth constraints with Zigbee and UWB, finally achieving a networked sensor platform. Additionally, using the standard ethernet physical layer enabled extremely precise time synchronization using Precision Time Protocol (PTP) [52]. However, the wired data channel required running signal cables even in harsh environments like the pig pen where Figure 2c is installed. This hard-wired setup turned out to be rather brittle once exposed to such environments, necessitating further evolution.

In order to deploy our vibration sensors in the pig farm, we needed a more robust and remotely manageable sensor network. To avoid the necessity of running data cables, we switched to a 2.4 GHz Wi-Fi radio based on an off-the-shelf ESP8266 microcontroller [40]. This iteration, shown both enclosed and with separate internals in Figure 2d, borrowed the geophone interfacing from the original hardwired prototype board in Figure 2a, but interfaced it with a stackable series of microcontroller "shields" [47] to enable remote data collection and deployment. While effective for many scenarios, this hardware stack was still overly sensitive to electrical noise and required manual amplifier control.

After the reliability issues with earlier pig farm sensors in Figure 2c and d, we built from that design to create a version dubbed "GeoESP8266v2.1", as shown in Figure 2e. This version integrated the analog processing chain onto a single printed circuit board (PCB) which then served as a carrier for off-the-shelf power supply and communication circuits. Unfortunately, a major drawback of this design was decreased flexibility since the vibration data could only be accessed remotely over the Wi-Fi channel, with no option for hardwired or local recording. This version finally introduced a digitally controllable amplifier circuit, though the range of available

gains was very limited with only 8 positions. With improvements in noise sensitivity and networking, this design was able to operate for several weeks to months in a harsh pig farm environment as described in Section 6.1. However, noise improvements were still needed in order to sense extremely low Signal-to-Noise Ratio (SNR) signals such as heartbeats and other biorhythms.

Across several iterations we built a more integrated and noise resistant version with a wider gain adjustment range, now termed *GeoMCU*. While still utilizing the same ESP8266 microcontroller as the previous few versions, we expect to eventually replace it with a more modern and better-supported System-on-a-Chip (SoC). Version 2.6, a minor variation from the current 2.7, is shown in Figure 2f with power supply, communication, and analog processing circuity all integrated directly on the same PCB. Unfortunately, version 2.6 suffered from a standardization issue with the wired output port, making most standard BNC connectors incompatible. With that issue resolved, the current iterations are highly flexible, due to a combination of dramatically increased gain adjustment range and the option for hardwired access to the raw geophone signal for deployments requiring high precision or a fast sample rate.

3 *GeoMCU* Design Overview

The *GeoMCU* system consists of an open-source PCB and two pieces of associated software, all connected in a sensor network. The PCB interfaces with a geophone transducer [74] to collect ground vibration and provides signal output via a hardwired analog connection or wirelessly from an onboard Analog to Digital Converter (ADC). On the PCB is a wireless ESP8266 SoC which runs custom firmware, comprising one of the software components. The remaining software component connects to the same wireless network with the sensor devices to receive and aggregate wirelessly transmitted data. These three components will be detailed in Section 4 while this sections focuses on the design principles at play in *GeoMCU*'s development.

Our design decisions for *GeoMCU* were primarily driven by the needs for our pig sensing project [11, 17], since it encompasses the most core challenges faced in the various deployment scenarios we explored. These challenges included:

- The need to detect very small signal changes such as heartbeats and other biorhythms in a high-noise environment.
- Limited access to the sensor nodes while the pig pens were occupied.
- The harsh environment below the pig pens, where the sensors are mounted, leads to unavoidable instability and potential damage.

More details on this application will be referenced later in Section 6.1, but the primary design goals we settled on for *GeoMCU* are:

- Low electrical noise, in order to enable sensing of small vibration signals such as those from heartbeats
- Remotely and precisely adaptable amplification, enabling adaptation to different sensing tasks, even when physical access to the devices is infeasible
- Resilience to hardware failures and software instability, both of which are common in harsh environments such as the underside of a pig pen

While focusing on this application's needs, we still preserved the flexibility to adapt to other scenarios such as indoor footstep sensing and human health monitoring.

3.1 Design Principles from Lessons Learned

Integrated PCBs have less noise. While hand-wired prototype boards are convenient for testing and on-the-fly builds, they are both brittle and prone to noise. By integrating the entire board onto a single PCB, manufacturing is more consistent and the layout can be optimized to reduce noise. This layout optimization includes separating the analog, digital, and power supply sections of the board to reduce coupling between them. Additionally, the most sensitive signal traces can be routed away from noisy components and power supply traces as well as being shielded by ground planes and "vias" [18].

Component choice contributes to noise reduction. While integrating the boards has benefits to noise reduction, the choice of components, particularly those in the noisier digital and power supply sections, can also play a role [18]. For example, by choosing a switching regulator with a frequency well above the analog chain's critical frequency band (in this case 10 Hz to 240 Hz), the noise generated from it can be readily filtered out. The multi-stage power supply design also helps to reduce noise, with the switching regulator performing most of the voltage conversion and a linear regulator providing the final conversion to 3.3 V for the digital and analog sections.

Check component tolerances, then plan for failures anyway. Several pitfalls we ran into with earlier versions came from electrical parts operating at the limits of their specified operating ranges. In particular, the digital potentiometers used for amplifier gain control have a limited functional range for their voltage inputs. However, even with careful tolerance checking, unexpected variations still occur in manufacturing and the demands from real-world sensing environments, necessitating workarounds and backup plans. In the case of *GeoMCU*, we found that due to manufacturing variations, some of the potentiometers will exhibit unstable behavior at moderately high gain settings. We work around this by testing each PCB individually once received from the manufacturer to see whether it will operate in this unstable regime, and use these boards only for sensing tasks which require less signal amplification, such as footstep detection.

Use common, standard parts, including generics where possible. While newer electronic components may claim performance gains, they are often more sensitive to heat and static discharge than long-tested, generic ones. These challenges lead to PCB manufacturing difficulties and result in failures which are difficult to reproduce and debug. Essentially, no matter the theoretical performance gains from more specialized parts, if the part can't be reliably soldered to the board, then no potential improvements in precision, noise, or power consumption can be realized. Additionally, availability challenges, such as the chip shortage from the COVID-19 pandemic, have greater impact on such newer components. Picking common

components that use standard pin layouts means that they can be easily swapped out for nearly equivalent parts as needed, further improving the reliability and manufacturability of the design.

Standards compliance improves reliability. This lesson relates to the previous in terms of hardware components, but also encompasses communication protocols and hardware. On the communication side, some of our earlier sensor versions attempted to use UWB and Zigbee radios for data transmission, but were thwarted by bandwidth constraints and radio incompatibilities. While Zigbee's physical layer is standardized [54], compatibility issues were widely prevalent at the time to the looser standardization of the higher layers [2]. However, standard Wi-Fi protocols [53] are so widely used and interoperable they can be relied upon even if individual components or commodity devices need to be replaced. The trade-off, of course, is increased power consumption for the Wi-Fi radio, necessitating multiple system configurations depending on the needed run time as described in Section 5. The combination of standardization and bandwidth constraints are why *GeoMCU* boards use Wi-Fi for the wireless data channel as opposed to a less power-intensive radio interface.

Ease of hardware use benefits both end users and developers. Since *GeoMCU* is designed to be used in a wide variety of environments, it needs to be easy enough to use for even non-technical users [15]. Quality-of-life features such as the wireless command line interface improve the ease of debugging and configuration both for such end users and for the engineers developing and debugging the hardware and firmware. While including features such as line editing and backup control interfaces increases development time, they ultimately improve the reliability and applicability of the whole system by easing debugging and configuration.

Time synchronization is useful, but not always necessary. On the surface, time synchronization seems like an obvious requirement for any sensor network where multiple sensors have overlapping sensing range. With the our original wired interface (Figure 2a), this issue was mitigated by using a centralized data acquisition unit for all data sampling. In the wireless regime, time synchronization between the sensor nodes induces a tradeoff in bandwidth, power consumption, and reliability. The synchronization operations consume power and bandwidth, and require individual sensor nodes to maintain time with each other even amidst network degradation and hardware failures. However, the analysis for many sensing tasks using *GeoMCU* can be easily adjusted to account for minor time synchronization errors (on the order of 1 s) [11, 20, 34, 39]. Thus, we relax the reliability and bandwidth constraints in *GeoMCU* boards by placing the timekeeping burden on the centralized data aggregator (see Section 4.3). For applications needing high-precision time synchronization such as vital signs monitoring and footstep localization [18, 24], *GeoMCU*'s wired configuration (see Section 5.3) can be employed with centralized data acquisition similar to our early prototype geophone interfaces.

A single flexible design is more useful than several fragmented ones. Up until the development of *GeoMCU* version 2.5, we continued using the original hand-wired prototype boards for controlled lab testing since there was insufficient flexibility in the earlier networked geophone hardware. The end result of this situation is that lab-bound use cases remained noisy and unreliable even as our networked interfaces were improving on those same metrics. By designing *GeoMCU* to account for both types of use cases, the lessons learned and iterative improvements from one deployment contribute to performance in other sensing tasks, ultimately improving reliability, signal quality, and usability across a wide range of sensor deployments.

4 Open Source Hardware and Software Components

The uniquely designed components of *GeoMCU* include the physical hardware board, its firmware, and the data aggregator software used for wireless data collection. This section will describe each of these components in turn, including the key design decisions in each.

4.1 Hardware

The primary *GeoMCU* board is designed to reduce electrical noise, increase resilience and recoverability, and expand flexibility across many potential sensing tasks. The open-source PCB design, created using KiCad [56], can be found online at https://github.com/NohPei/GeoMCU. Within the board, there are three sections to improve electrical noise characteristics: one for power supplies, one for digital communication, and one for analog signal handling. These three sections are separated by wide channels (shown in Figure 3, highlighted in Figure 4b) to reduce electrical interference. The large empty space in the upper left corner of Figure 3 is a reserved area for the geophone transducer when the PCB is installed in an enclosure. The conductive material is removed near the geophone to prevent interference from the geophone's magnetic field. While the power and digital sections are fairly conventional, the analog section contains the most careful design choices to achieve our goals with *GeoMCU*, which we highlight in Figure 4.

GeoMCU's power supply section is based on the application circuit for a common buck converter [3]. The power input is designed for 12 V but can accept anywhere from roughly 6 V to 24 V, depending on the tolerance of the input capacitor. The switching regulator decreases the input voltage to 5 V before a standard linear regulator performs the final conversion to the 3.3 V needed by the digital and analog sections. This two-stage process improves efficiency and noise in tandem by performing most of the voltage drop in an efficient switching regulator while the final linear regulator absorbs much of the switching noise. Component choice also plays a role in noise reduction, ensuring the switching frequency of the buck converter stage is well above the 10 Hz to 240 Hz sensitivity range of our geophone transducers [64].

For digital communication and control, *GeoMCU* includes an ESP8266 microcontroller [40]. While newer and more capable SoCs are available, the current iteration of *GeoMCU* uses this chip for its low cost and long-tested reliability. The microcontroller controls the onboard amplifier and ADC while communicating wirelessly to transmit collected sensor data and receive configuration updates. The ADC and gain control chips interface with it via a standard serial peripheral interface (SPI) bus, providing fast and precise data transfer to the host controller.

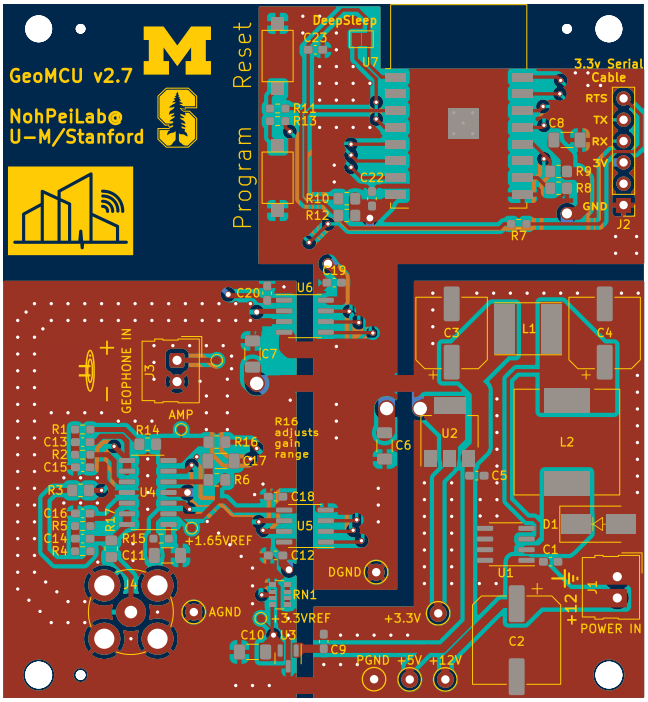

Figure 3: Design drawings of the *GeoMCU* PCB showing the full layout. Wide channels divide the three sections: power (lower right), digital (upper right and center), and analog (lower left). An empty space in the upper left corner is reserved for the geophone itself.

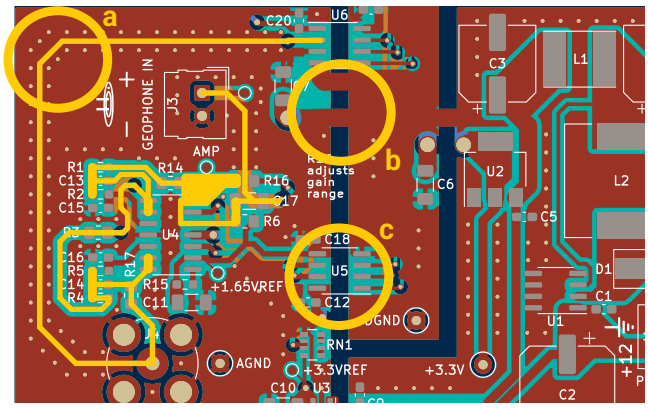

Figure 4: A zoomed-in view of the Analog section of the *GeoMCU* PCB with the geophone signal path highlighted in yellow. Three circles highlight key layout and design points: (a) shielding analog signal traces using ground planes and vias, (b) separated board sections to reduce noisy crosstalk, (c) the digital potentiometer used for precise and remote amplifier gain control

GeoMCU's analog circuitry for raw signals necessitates the most careful design to ensure adaptability and reduce electrical interference. The geophone input connects to an amplifier circuit controlled by a digital potentiometer (Figure 4c), which facilitates amplifier adjustment and remote control. An active filter circuit follows to reduce sampling artifacts and high frequency noise. Output from the filter is routed to the analog output port as well as the sampling ADC, enabling data collection from either path. Throughout the analog section, we shield the signal trace as much as possible by surrounding it with grounding planes and conductor-plated through holes (i.e., "vias"), as shown in Figure 4a.

4.2 Sensor Firmware

The firmware running on *GeoMCU*'s microcontroller uses the Arduino framework [4] but is typically compiled using PlatformIO [72]. Arduino enables an easy, predictable development process for various microcontrollers, but can struggle with library management and compilation tools between different computers. PlatformIO works with the Arduino framework, while offering more consistent library management and environment setup. The firmware source code is open and available on GitHub at https://github.com/NohPei/geoscope-sensor, and build instructions can be found in the included `README` or in the user manual at https://geomcu.readthedocs.io.

We focus on resilience in the firmware design, aiming to recover quickly in the expected event of temporary failures in individual sensor nodes. Essentially, this means responding to any errors or unexpected code paths by immediate reboot while minimizing the startup time to reduce the resulting delays and missed data. To support this approach, we offload processing to external devices rather than performing any on the *GeoMCU* nodes themselves, as shown in Figure 6. This keeps the nodes simple and less prone to error while enabling fast reboot times, minimizing the impact of faults, and reducing recovery latency. The key idea is that whenever errors and faults occur, we recover as quickly as possible to a known good state, restoring the sensor to operation.

The firmware includes a command-line interface accessible by serial port or through a Wi-Fi network via the standard `telnet` protocol. This interface allows for explicit configuration of amplifier gain and sample rate as well as the networking configuration for Wi-Fi networking, IP addresses, and the MQTT messaging protocol which handles data passing between sensor nodes and data storage [5, 11]. Additionally, the interface is useful for debugging the PCB and firmware itself by enabling manipulation during testing and direct access to the sampled data before it is sent to the MQTT broker. Thus, including the command-line interface mitigates many of the deployability and ease-of-use challenges of earlier iterations.

4.3 Aggregator for Wireless Data Collection

Since the *GeoMCU* sensors are able to communicate wirelessly, host-side software is needed to aggregate the data for later processing in such configurations. As with the other *GeoMCU* components, the source code is openly available on GitHub at https://github.com/NohPei/geoscope-gateway. The aggregator runs as an asynchronous Python program, receiving data packets over MQTT from individual nodes and periodically recording them to disk in JavaScript Object Notation (JSON) format. While inefficient for time series data, JSON is an easily readable and widely supported file format, making it a good choice during setup and troubleshooting. If scalability necessitates in the future, the format can be readily

replaced with more compact formats by making minimal changes to the aggregator software and sensor firmware. The asynchronous programming model allows for scalability to large numbers of *GeoMCU* nodes with minimal additional resource usage.

To enhance overall system resilience, the data aggregator handles timestamping under the assumption that individual sensor nodes are unreliable. Our current sensor firmware has no time synchronization on its own, since such would be disrupted by sensor reboots employed for resilience and error recovery. Past attempts to incorporate time synchronization have led to either unreliability or excessive communication overhead, ultimately preventing use of the data channel for sensor networking. Thus, the data aggregator records timestamps provided by the sensors if they are included, but also logs the time each data packet is received. While this "receive time" timestamp is only as precise as transmission and processing time, it ensures that a consistent time basis is used for all received data, even if sensor restarts occur.

5 *GeoMCU* as a Sensor Network

For most structural vibration sensing tasks an individual *GeoMCU* node is insufficient, so several are connected in concert to collect vibration data at separate locations. This section will describe how *GeoMCU* nodes can be connected into a sensor network, including common hardware configurations in which they can be deployed and an overview of the components required for building such a network.

Sensor data from individual *GeoMCU* nodes can be collected either wirelessly (via MQTT over the Wi-Fi data channel) or hardwired (through the analog output port). Using the analog port, the sensor data can be recorded using any off-the-shelf data acquisition unit, enabling high precision and high sample rate for applications that need it, such as localization and vital signs monitoring. Over the wireless channel, a 12-bit ADC with configurable sample rate captures sensor data and ferries them over the Wi-Fi network as MQTT packets. The sample rate is typically set to 500 Hz to match the Nyquist rate for the geophone's sensitivity range of up to 240 Hz. The individual sensor notes connect to an MQTT broker which distributes sensor data packets to the data aggregator or any future software developed to interact with these sensors in real time.

Individual *GeoMCU* nodes can be flexibly powered in a few different ways. For longer-term deployments or lab use, the sensors are built for a 12 VDC input, although that can vary anywhere from as low as 9 V up to approximately 24 V where the input capacitor maxes out. To enable fully wireless operation an increase portability, the 12 V supply can be provided by a standard Lithium Polymer (LiPo) battery such as those used for hobby aircraft and drones. In testing, we found that a typical 3S LiPo battery can power a *GeoMCU* board continuously for at least 24 h depending on sample rate and Wi-Fi transmission distance.

For wireless data transfer and control, the sensors connect to a commodity 2.4 GHz Wi-Fi network and connect to an MQTT broker. While data collection using the analog output port should not strictly require the network connection, we recommend still connecting the sensors to the network for control, configuration, and stability purposes. The MQTT broker receives packets of sensor data from the onboard ADC for distribution to data aggregator along with control messages to route to individual sensors. Theoretically, any standards-compliant [7] message broker could be used, however we universally use a local MQTT broker such as the open source Eclipse Mosquitto [58] since the *GeoMCU* firmware is not configured for an encrypted broker connection. Using a local broker also reduces potential for information leakage which may be crucial for some sensing scenarios such as health monitoring.

To protect the individual sensor nodes, they are designed to fit in a watertight enclosure, specifically a Bud Industries PN-1323 [55] box. While the bare PCB is sufficient in controlled environments, any outdoor or harsh environment usage necessitates waterproofing. Additionally, our deployment experiences in pig farms revealed that water resistance alone is insufficient since common sealing materials are degraded by components of animal waste such as urea [39]. For most outdoor and animal monitoring scenarios, the chosen enclosure is resistant to these common chemical hazards, though adaptation may be needed if future deployments are undertaken in more caustic environments.

We architect networks of *GeoMCU* sensors by considering individual sensors nodes unreliable. This assumption stems primarily from the experiences of the pig farm deployment, were even fully encapsulated sensors have intermittent power and connection challenges along with occasional total failure due to leakage or damage. Thus, we offload the time synchronization to the data aggregator layer (for wireless setups) or data acquisition card (for wired setups) to reduce the individual sensors' computation, communication, and complexity overhead, as discussed in Section 4.3. Since many of our sensing applications process separate sensors individually [9, 11, 34, 39, 46] before combining them, we find the imprecise timestamps from the data aggregator acceptable for situations where our sensors are communicating wirelessly. When high precision time accounting is needed, such as for localization [38, 45, 64], the analog output port provides the option for time synchronization by the external data acquisition unit.

(a) (b) (c)

Figure 5: *GeoMCU* Sensors in several common hardware configurations: (a) Water tight, power wired for long-term deployment; (b) Fully wireless, battery powered for outdoor deployments; (c) fully wired configuration for high-precision in controlled environments

5.1 Water-Resistant Configuration for Long-Term Monitoring

For long-term monitoring scenarios, such as our pig farm deployments [11, 39], we deploy water-protected *GeoMCU* sensors with hardwired power supplies. A set of these fully encapsulated sensors

is shown in Figure 5a, soon before they were installed beneath the pig pens. There is a reliability trade-off in this configuration due the hole drilled for an external power connector. However, our encapsulation and recoverability efforts make this acceptable for the scenarios we have used it for so far. Using this configuration, *GeoMCU* deployments at a pig farm site have been operating nearly continuously for over 3 years as discussed in Section 6.1.

The sensors are wired for power despite the potential challenges with animal interference because of the need for long-term deployment. While long-term deployments with battery-powered or self-powered devices are an area of active research [73], the continuous sampling requirement needed for exploratory vibration sensing precludes the use of such techniques in *GeoMCU* so far. Thus, for any deployment longer than approximately 24 hours our *GeoMCU* sensors need an external power source. We did note interference by the animals with this wired power configuration in one early experiment in a pig farm [11]. Fortunately, with better cable placement and proper chemical resistance the risk of interference to the power supply can be largely mitigated [17, 39].

In these deployments, the sensors are typically concentrated in a relatively close area, enabling a simple star topology for the network configuration. This means we deploy a single Wi-Fi access point for all the sensors to connect to, as shown in Figure 6. A computer hosting the MQTT broker and data aggregator is connected to the same network through cable or its own Wi-Fi connection. While there is a potential failure point in this centralized topology, the ability to use commodity off-the-shelf devices and separate them from the worst of the environmental hazards reduces this risk.

For both data back up and reliability, we regularly ferry sensor data off-site from the aggregator computer over any available internet connection. Since this configuration is typically used to remote environments such as farms and outdoor event spaces, this typically means a cellular network. Where more reliable outgoing connections are available they can absolutely be utilized, however these scenarios typically have unreliable infrastructure if any traditional networking is available at all. By sending the data off site, we improve the overall sensor network's reliability since data is preserved until the last backup even in the event of total system failure.

In wireless configurations, the *GeoMCU*'s sensor network reliability is split between individual sensor nodes, the intermediate data aggregator, and off-site data processing. Figure 6 shows this network map, with the least reliable device being individual *GeoMCU* sensors, followed by the local data aggregator, and finally remote storage and processing. We note a link between reliability and processing capability in this setup, with more capable devices also engendering increased reliability. This can be explained by both increased distance from potential hazards and increased capability to self-monitor.

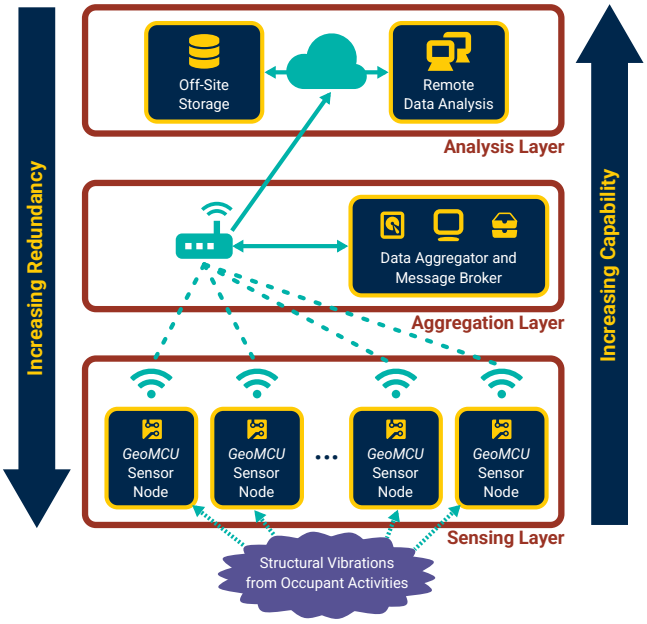

Figure 6: A network map for *GeoMCU* in the long-term water-resistant configuration, divided into three tiers of reliability: the sensing layer is the least reliable and therefore has the most redundancy, while the aggregation layer is still low-powered, but more reliable than the individual sensors. The analysis layer is off-site to maximize reliability and processing capability.

5.2 Fully Wireless Mesh Configuration for Outdoor Deployments

For larger area and outdoor projects, such as in sports stadiums, we use fully enclosed *GeoMCU* sensors in a wireless mesh, powered by batteries. The mesh network enables a much wider deployment area since individual sensors do not need to be within range of a single radio, with a trade-off of more potential failure points with data packets being passed back and forth between wireless nodes.

This network architecture operates very similarly to the fully wired setup, but is limited in duration by the need for battery power. As before, the MQTT broker is connected to the same network with the rest of the sensor nodes and they send their data packets to it for aggregation. The most major difference is that data transmission time between individual sensors and the broker computer is highly variable due to the mesh topology. For example, while stadium deployments are typically laid out in a ring, the access points are free to connect to one another directly across the playing area if range permits. While this tradeoff does introduce additional uncertainty in the data timestamps, that can be mitigated with less time-sensitive processing algorithms.

Various mesh communication technologies could be utilized in this scenario, however our previous development experience led us to a standards-compliant 802.11s Wi-Fi mesh. Rather than individual sensor nodes connecting directly, the sensors connect to standard access points which then mesh with one another for wireless backhaul. The benefit of this approach is that sensor nodes need not be powerful enough to handle each other's traffic, and the access points can be easily replaced commodity hardware. By offloading the mesh organization and forwarding to the Wi-Fi access points, the *GeoMCU* sensors can preserve their low power, low computation, and limited reliability while still enabling communication over larger distances than a star topology can provide.

5.3 Fully Wired for High-Precision Indoor Scenarios

The analog output port enables *GeoMCU* to be used for applications requiring high sample rates or higher sensing resolution than the on-board ADC can provide. Using the wireless connection, time synchronization is limited to that provided by the data aggregator's timestamping and sample resolution is limited to 12 bits. However, with the analog output we can utilize *GeoMCU*'s filters and amplification as a front-end to an external data acquisition unit similar to those used for industrial accelerometers.

For these deployments, the name boards operate very similar to the original boards shown in Figure 2a, but with drastically reduced noise and more fine-grained control over the amplification. Power can be supplied by a standard 12 VDC power supply, and the analog output is connected to a data acquisition unit. Note that while sensor data is not strictly being collected via the wireless channel, the *GeoMCU* sensors should still be connected to a Wi-Fi network and MQTT broker for control, configuration, and maximum stability. This configuration enables high-precision applications in controlled environments to take advantage of *GeoMCU*'s noise reduction from the integrated and carefully laid out analog circuitry. The analog output port is a common BNC connector for compatibility with other scientific equipment.

6 *GeoMCU* Real-World Evaluations

Since we designed *GeoMCU* for general structural vibration sensing applications, we have been able to apply it to a wide variety of scenarios and sensing tasks. This section will present evaluations of *GeoMCU*'s efficacy as demonstrated in four different real-world deployment scenarios which we have conducted over the past few years. For further detail on these deployments, please refer to the original papers published on each of these topics, which are cited throughout this section.

6.1 Pig Farm Monitoring

Precision livestock management is important to improve the health of farm animals and enhance productivity in the agricultural industry. In this section, we will discuss the deployment of *GeoMCU* for automatically monitoring the growth of piglets and health of their mothers over the pre-weaning cycle. This period is crucial to improve the survival rate of newborn pigs, which averages only 87% [11, 20, 39]. By evaluating *GeoMCU*'s performance at these tasks, we demonstrate the quality and efficiency of data which *GeoMCU* can collect as well as its resilience to long-term deployment challenges.

As discussed in Section 3, our pig farm deployments was one of the key driving examples for developing *GeoMCU*. After several hardware iterations, such as those shown in Figure 2e and Figure 2f, we've now deployed *GeoMCU* nearly continuously for over 3 years at the USDA's Meat Animal Research Center in Nebraska, USA. With such a long-term deployment we have been able to evaluate *GeoMCU*'s longevity and error recovery capability, as shown in Figure 7. In short, as we have improved both the hardware protection (see Section 5.1) and recovery mechanisms (see Section 4.2), we have seen the MTBF for permanent sensor failures rise from just under 1 week to well over a year for the most recent deployment.

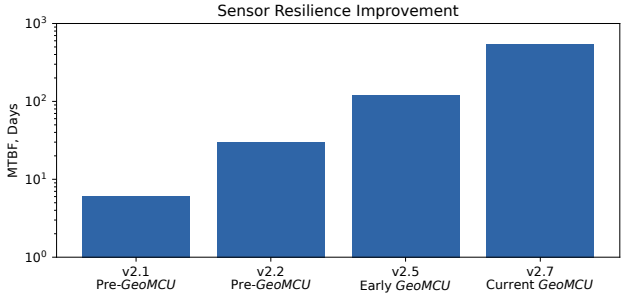

Figure 7: A chart showing *GeoMCU*'s resilience improvement over several hardware iterations. Each bar represents a different hardware version, including two previous hardware platforms and two iterations of *GeoMCU*'s design. The vertical axis shows the Mean Time Between Failures (MTBF) in days on a logarithmic scale since the most recent version has only had 3 failed sensors in 2 years.

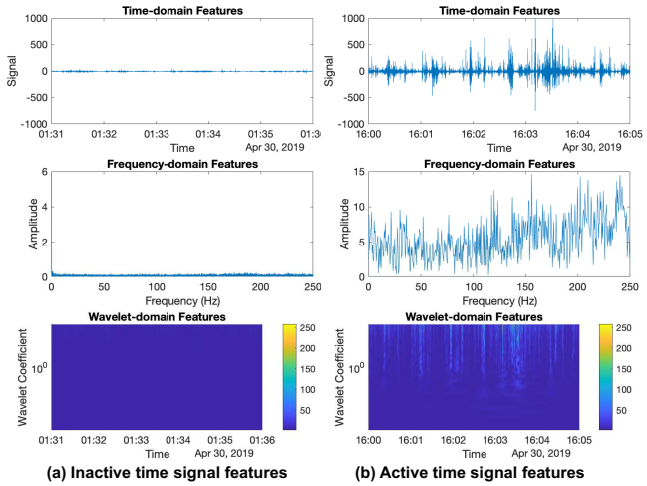

Figure 8: Pig farm monitoring data samples and their features in the time, frequency, and wavelet domains. Samples are extracted times of day when the pigs are alternately (a) resting and (b) highly active.

During times that pigs are active, there are significant fluctuations in the structural vibration signal which correspond to variations in pig activity. Figure 8 shows an example of the data collected from the pig farm, providing an overview of time-, frequency-, and wavelet-domains of the vibration signal during active and non-active times of the pig activities. By analyzing the signals and modeling the features extracted from time- and frequency- domains, such as the mean signal amplitude per 10Hz-frequency range, the data enables the classification of various activities such as posture and transitioning monitoring (with 97.8% and 94% accuracy, respectively), ingestion and excretion detection (with 96% and 71% accuracy, respectively), and piglet nursing, sleeping, and active

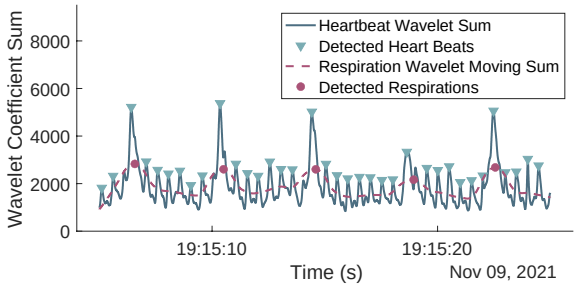

Figure 9: Heartbeats (triangle markers) and respirations (circle markers) are detected in the vibration signals when the pig is lying still.

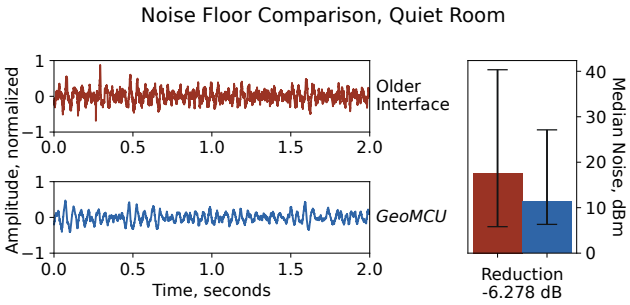

Figure 10: A comparison of vibration data collected by an earlier geophone interface and *GeoMCU*'s updated sensor boards respectively. The newer board decreased baseline noise in the vibration signal by over 6 dB, including having filtered out the high frequency spike near the 0.25 s mark.

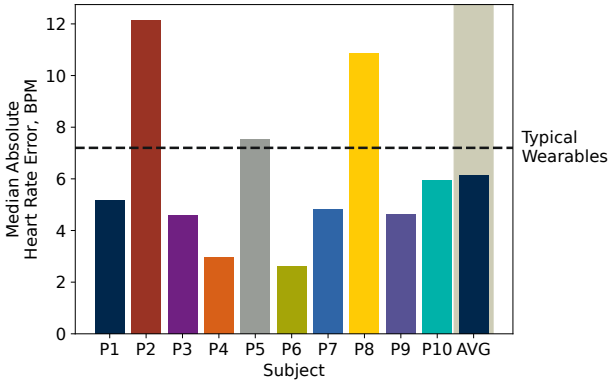

Figure 11: Heart Rate Accuracy using *GeoMCU* sensors and an optimized heart rate detection algorithm. Each bar represents a different subject, with the final grouping is averaged across all 10 subjects to show overall performance. Typical heart rate accuracy for wearable sensors is shown for comparison.

time detection (with 87.7%, 89.4%, and 81.9% accuracy, respectively). As compared to traditional computer vision studies, our vibration-based approach requires 12× less storage and 4× less training time than the vision-based approach trained on Resnet18 [17, 49].

During inactive times, the pigs produce very little vibration, which enables monitoring more fine-grained signals. As shown in Figure 8a, the vibration signal amplitude is close to zero which allows the detection of Heart Rate (HR) and Respiration Rate (RR), since our *GeoMCU* system is highly sensitive [20] and our sensors are in close proximity to the pigs' bodies [39]. A zoomed-in view of the pig's heart beats and respiration rhythm is visualized in the wavelet domain in Figure 9, where the pig's respirations are identified as periodic fluctuations in the heartbeat vibration amplitude.

6.2 Human Heart Rate Detection

Heart Rate (HR) is one of the most basic metrics of human health, and ubiquitous monitoring is particularly important for early detection of potential disease. Typical heart rate monitoring methods require direct body contact, have privacy issues, and/or are limited in their scalability [18]. By using our *GeoMCU* sensors, we instead monitor heart rate by detecting the tiny vibrations caused by heartbeats. The key challenges are the extremely low SNR caused by other vibration sources and variations in heartbeat vibration signals between individual people.

Since heartbeat-induced structural vibrations have such small SNR, we use *GeoMCU* in its wired configuration for maximum precision and dynamic range, as described in Section 5.3. As previously mentioned, one of *GeoMCU*'s main contributions is a marked improvement in noise figure due to the careful choice of components and noise isolating PCB layout. In Figure 10 we show a comparison between the older, hand-wired geophone interface (Figure 2a) that would have been used for similar scenarios before developing *GeoMCU* and our most recent iteration. When measuring the background vibration in a quiet room, we see a as you can see when measuring the background vibration in a quiet room we see a 6 dB (or 4×) decrease in the ambient noise, enabling detection of heartbeat-induced vibrations which were previously below the noise floor.

To evaluate our *GeoMCU* boards on actual heart rate monitoring, we collected vibrations with 10 different individuals of varying health, sex, and age. Figure 11 shows that across all 10 individuals and three potential sensor locations, we are able to monitor heart rate within 7 bpm (beats per minute) on average, and below 5 bpm for most individuals. There is some variation between individuals due to individual subjects' health conditions [18], but even in the worst cast median heart rate error remains below 12 bpm.

6.3 Crowd Monitoring in Stadiums

Monitoring crowd behavior and activity levels in public spaces is useful for both enhancing public safety and improving the experience of attendees at large events. We have deployed *GeoMCU* sensors in a wireless mesh configuration (see Section 5.2) at multiple sports games both indoors at Stanford's Maples Pavilion [34], and outdoors at Michigan Stadium [12, 13, 33]. The vibration sensors collect the structural vibrations induced by crowd activities such as clapping and cheering. By monitoring these vibrations, we

are able to detect the crowd's reactions to game events, including how they react to different teams scoring and promotional events.

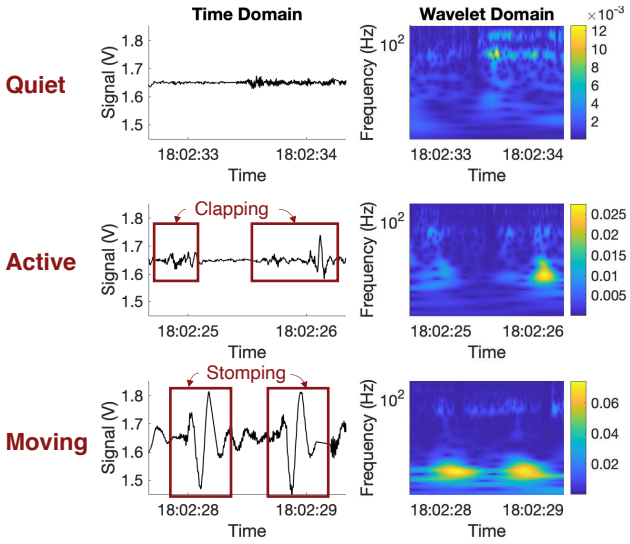

Figure 12: Three plots showing crowd vibration data collected by *GeoMCU* during periods of quiet, clapping, and stomping. Both time domain and wavelet domain plots are included to highlight the separability of these different activity types in both frequency content and amplitude.

To evaluate *GeoMCU*'s usefulness in monitoring these crowd vibrations, we did some characterization on what activities could be detected. Figure 12 shows examples of vibration data in both the time and time-frequency (i.e., wavelet) domains as measured during periods of quiet, clapping, and stomping. As can be seen, different crowd activities can be differentiated by both amplitude and frequency content, enabling robust crowd reaction detection using *GeoMCU*'s structural vibration sensing. By combining this data with facility models and game event information, we were able to achieve a 90% F1 score in detecting crowd reactions a 9.3 person Mean Absolute Error (MAE) in estimating crowd traffic [34].

6.4 Human Gait Health Monitoring

Footstep-induced floor vibration captured by sensors like *GeoMCU* has demonstrated promising performance among various gait health and footstep monitoring tasks [42, 43, 44, 45, 62, 63, 67, 68, 69, 70]. In this context, gait refers to the details of a person's walking, including their balance, footstep timing, and other metrics [28]. Gait health monitoring is essential to assessing risk of trips and falls [25, 35, 69], tracking the development of neurological disorders (e.g., Parkinson's and strokes) [14, 30], and tracking rehabilitation and progression of musculoskeletal disorders (e.g., arthritis and muscular dystrophies) [24, 27, 38].

When an individual is walking, as in Figure 13a, each footstep exert forces onto the floor that generates vibrations, which *GeoMCU* sensors can detect. The analysis of these vibration signals allows inference on an individual's postural balance, left-right symmetry, joint movements, and joint force/moment transmissions related to

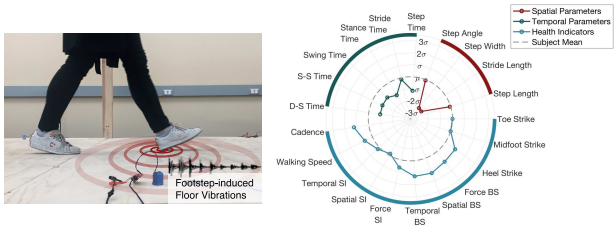

(a) Footstep floor vibrations **(b) Personalized gait profile**

Figure 13: *GeoMCU* captures the floor vibrations generated by footsteps during walking (a), which produce estimates of spatial, and temporal gait parameters and gait health indicators (b).

an in individuals' overall physical health status. Figure 13b shows an example of a personalized gait profile generated from our vibration-based gait parameter estimation model. The visualization allows clinicians and individuals to understand gait health as compared with the average gait from a normative baseline (gray dashed line around the center).

Our prior studies have leveraged *GeoMCU* to sense subtle changes in footstep-induced floor vibrations to conduct in-clinic and in-home gait analysis that matches the standards of clinical requirements. These results include identifying walkers with >90% of accuracy among 10 people [21, 23, 37], estimating spatial and temporal gait parameters with <5% of error rate [29, 30], detecting gait abnormalities through subtle changes in foot-floor contacts with up to 92% accuracy [25, 35, 36], and estimating joint angles and ground reaction forces with comparable performance with wearable sensors based on inertial measurement unit (IMU)s [26, 43]. A recent deployment at Nationwide Children's Hospital shows success (94.8% accuracy) in tracking disease progression stages for children with muscular dystrophy [24, 38]. These results demonstrate the promise of *GeoMCU* as a gait health monitoring platform.

7 Related Work

Most vibration sensing work uses accelerometers instead of the geophones we use with *GeoMCU* [19, 48, 61, 65, 78]. While ubiquitous, accelerometers use higher frequency ranges which are attenuated more rapidly in solid structures [69]. Additionally, typical accelerometers exhibit much higher noise characteristics due to their integrated microelectronic design. Thus, accelerometers are useful over short distances but are less effective for many of the ubiquitous structural vibration monitoring applications *GeoMCU* is used for.

While other geophone interface systems exist, most are designed for seismic monitoring instead of structural vibrations [6, 50, 77]. These typical geophone interfaces are inserted into soil or rock to intermittently measure earthquake activity. Since earthquake amplitude is relatively large, these devices require little amplification or adaptability and thus can operate autonomously for long periods of time with little power consumption. However, the health and activity monitoring applications *GeoMCU* is designed for require

adaptable amplification and more continuous measurement in order to capture to faster-changing and smaller-amplitude vibrations from human and animal movements.

Many other sensing transducers use embedded wireless interfaces similar to *GeoMCU* [61, 73]. These interfaces include a variety of wireless protocols power, power supply mechanisms, and computation capabilities. *GeoMCU* draws on lessons learned from these previous platforms, optimizing for our goals of adaptability, low noise, and resilience.

8 Conclusion

We have presented *GeoMCU*, a resilient, low-noise geophone sensing platform designed for structural vibration sensing in a variety of environments. Through an iterative design process and lessons learned from previous sensor deployments, we have presented principles for designing a sensor network that is resilient, adaptable, and low noise. Applying these principles, we showcased the unique hardware and software components of *GeoMCU*, along with orchestration of *GeoMCU* as a sensor network. Through deployment experiences in varied scenarios, we demonstrated *GeoMCU*'s improvements in resilience, adaptability, and noise reduction, including a 4× reduction in background noise and greater than 10× improvement in average time between sensor node failures.

By continuing to develop and share our designs, we hope to continue to improve the state of the art in structural vibration sensing. With further ease of use, modernization, and deployability efforts, we envision *GeoMCU* as a cornerstone in a widely applicable Internet of Structures, enabling numerous applications in health, safety, and activity monitoring.

References

[1] Jatin Aggarwal, Jingxiao Liu, and Hae Young Noh. 2023. Vehicle-invariant drive-by monitoring across multiple bridges through bootstrappingenhanced unsupervised domain adaptation. en. In *Proceedings of the 14th International Workshop on Structural Health Monitoring*. Structural Health Monitoring 2023. Destech Publications, Inc., (Sept. 12, 2023). ISBN: 978-1-60595-693-0. doi:10.12783/shm2023/36909.

[2] Mohab Aly, Foutse Khomh, Yann-Gaël Guéhéneuc, Hironori Washizaki, and Soumaya Yacout. 2019. Is fragmentation a threat to the success of the internet of things? en. *IEEE Internet of Things Journal*, 6, 1, (Feb. 2019), 472–487. doi:10.1109/JIOT.2018.2863180.

[3] 2015. AP1509 buck converter. en. Diodes Incorporated. (June 18, 2015). Retrieved July 10, 2025 from https://www.diodes.com/part/view/AP1509.

[4] [SW], Arduino 2006. Arduino LLC. URL: https://www.arduino.cc/Retrieved May 24, 2025 from.

[5] Sripong Ariyadech, Amelie Bonde, Orathai Sangpetch, Woranun Woramontri, Wachirawich Siripaktanakon, Shijia Pan, Akkarit Sangpetch, Hae Young Noh, and Pei Zhang. 2019. Dependable sensing system for pig farming. en. In *2019 IEEE Global Conference on Internet of Things (Gciot)*. 2019 IEEE Global Conference on Internet of Things (GCIoT). IEEE, Dubai, United Arab Emirates, (Dec. 2019), 1–7. ISBN: 978-1-7281-4873-1. doi:10.1109/GCIoT47977.2019.9058398.

[6] Hussein Attia et al. 2020. Wireless geophone sensing system for real-time seismic data acquisition. en. *IEEE Access*, 8, 81116–81128. doi:10.1109/ACCESS.2020.2989280.

[7] Andrew Banks, Ed Briggs, Ken Borgendale, and Rahul Gupta, (Eds.) 2019. *MQTT Version 5.0*. en. OASIS Standard, (Mar. 7, 2019). https://docs.oasis-open.org/mqtt/mqtt/v5.0/mqtt-v5.0.html.

[8] Amelie Bonde, Shijia Pan, Zhenhua Jia, Yanyong Zhang, Hae Young Noh, and Pei Zhang. 2018. VVRRM: vehicular vibration-based heart RR-interval monitoring system. en. In *Proceedings of the 19th International Workshop on Mobile Computing Systems & Applications* (HotMobile '18). HotMobile '18: The 19th International Workshop on Mobile Computing Systems and Applications. Association for Computing Machinery, New York, NY, USA, (Feb. 12, 2018), 37–42. ISBN: 978-1-4503-5630-5. doi:10.1145/3177102.3177110.

[9] Amelie Bonde, Shijia Pan, Mostafa Mirshekari, Carlos Ruiz, Hae Young Noh, and Pei Zhang. 2020. OAC: overlapping office activity classification through IoT-sensed structural vibration. en. In *2020 IEEE/ACM Fifth International Conference on Internet-of-things Design and Implementation (Iotdi)*. 2020 IEEE/ACM Fifth International Conference on Internet-of-Things Design and Implementation (IoTDI). IEEE, Sydney, Australia, (Apr. 2020), 216–222. ISBN: 978-1-7281-6602-5. doi:10.1109/IoTDI49375.2020.00028.

[10] Amelie Bonde, Shijia Pan, Hae Young Noh, and Pei Zhang. 2019. Deskbuddy: an office activity detection system: demo abstract. en. In *Proceedings of the 18th International Conference on Information Processing in Sensor Networks* (IPSN '19). IPSN '19: The 18th International Conference on Information Processing in Sensor Networks. Association for Computing Machinery, New York, NY, USA, (Apr. 16, 2019), 352–353. ISBN: 978-1-4503-6284-9. doi:10.1145/3302506.3312490.

[11] Amelie Bonde et al. 2021. PigNet: failure-tolerant pig activity monitoring system using structural vibration. en. In *Proceedings of the 20th International Conference on Information Processing in Sensor Networks (Co-Located with Cps-iot Week 2021)*. IPSN '21: The 20th International Conference on Information Processing in Sensor Networks. ACM, Nashville TN USA, (May 18, 2021), 1–13. ISBN: 978-1-4503-8098-0. doi:10.1145/3412382.3458902.

[12] Yen Cheng Chang, Jesse Codling, Yiwen Dong, Jiale Zhang, Jiasi Chen, Hae Young Noh, and Pei Zhang. 2025. Poster abstract: leveraging general-purpose audio datasets for vibration-based crowd monitoring in stadiums. en. In *Proceedings of the 23rd ACM Conference on Embedded Networked Sensor Systems*. SenSys '25: 23rd ACM Conference on Embedded Networked Sensor Systems. ACM, UC Irvine Student Center. Irvine CA USA, (May 6, 2025), 590–591. ISBN: 979-8-4007-1479-5. doi:10.1145/3715014.3724022.

[13] Yen Cheng Chang, Jesse Codling, Yiwen Dong, Jiale Zhang, Jeffrey Shulkin, Hugo Latapie, Carlee Joe-Wong, Hae Young Noh, and Pei Zhang. 2024. Poster abstract: listen and then sense: vibration-based sports crowd monitoring with pre-training with public audio datasets. en. In *2024 23rd ACM/IEEE International Conference on Information Processing in Sensor Networks (IPSN)*. 2024 23rd ACM/IEEE International Conference on Information Processing in Sensor Networks (IPSN). IEEE, Hong Kong, (May 13, 2024), 285–286. ISBN: 979-8-3503-6201-5. doi:10.1109/IPSN61024.2024.00043.

[14] Kylie Clewes, Claire Hammond, Yiwen Dong, Mary Meyer, Evan Lowe, and Jessica Rose. 2024. Neuromuscular impairments of cerebral palsy: contributions to gait abnormalities and implications for treatment. en. *Frontiers in Human Neuroscience*, 18, (Sept. 18, 2024), 1445793. doi:10.3389/fnhum.2024.1445793.

[15] Jesse R Codling, Amelie Bonde, Yiwen Dong, Siyi Cao, Akkarit Sangpetch, Orathai Sangpetch, Hae Young Noh, and Pei Zhang. 2021. MassHog: weight-sensitive occupant monitoring for pig pens using actuated structural vibrations. en. In *Adjunct Proceedings of the 2021 ACM International Joint Conference on Pervasive and Ubiquitous Computing and Proceedings of the 2021 ACM International Symposium on Wearable Computers* (UbiComp '21). UbiComp '21: The 2021 ACM International Joint Conference on Pervasive and Ubiquitous Computing. Association for Computing Machinery, New York, NY, USA, (Sept. 21, 2021), 600–605. ISBN: 978-1-4503-8461-2. doi:10.1145/3460418.3480414.

[16] Jesse R Codling, Mostafa Mirshekari, Hae Young Noh, and Pei Zhang. 2020. Demo abstract: active structural occupant detector. en. In *2020 19th ACM/IEEE International Conference on Information Processing in Sensor Networks (IPSN)*. 2020 19th ACM/IEEE International Conference on Information Processing in Sensor Networks (IPSN). IEEE, Sydney, Australia, (Apr. 2020), 353–354. ISBN: 978-1-7281-5497-8. doi:10.1109/IPSN48710.2020.00-10.

[17] Jesse R Codling et al. 2022. Sow posture and feeding activity monitoring in a farrowing pen using ground vibration. en. In *ECPLF 2022 - 10th European Conference on Precision Livestock Farming*. 10th European Conference on Precision Livestock Farming. Vienna, Austria, (Aug. 30, 2022).

[18] Jesse R. Codling, Jeffrey D. Shulkin, Yen-Cheng Chang, Jiale Zhang, Hugo Latapie, Hae Young Noh, Pei Zhang, and Yiwen Dong. 2024. FloHR: ubiquitous heart rate measurement using indirect floor vibration sensing. en. In *Proceedings of the 11th ACM International Conference on Systems for Energy-efficient Buildings, Cities, and Transportation* (BuildSys '24). BuildSys '24: The 11th ACM International Conference on Systems for Energy-Efficient Buildings, Cities, and Transportation. Association for Computing Machinery, Hangzhou China, (Oct. 29, 2024), 44–54. ISBN: 979-8-4007-0706-3. doi:10.1145/3671127.3698170.

[19] Dian Ding, Lanqing Yang, Yi-Chao Chen, and Guangtao Xue. 2021. VibWriter: handwriting recognition system based on vibration signal. en. In *2021 18th Annual IEEE International Conference on Sensing, Communication, and Networking (SECON)*. 2021 18th Annual IEEE International Conference on Sensing, Communication, and Networking (SECON). IEEE, Rome, Italy, (July 2021), 1–9. ISBN: 978-1-6654-4108-7. doi:10.1109/SECON52354.2021.9491615.

[20] Yiwen Dong, Jesse R Codling, Gary Rohrer, Jeremy Miles, Sudhendu Sharma, Tami Brown-Brandl, Pei Zhang, and Hae Young Noh. 2023. PigV2: monitoring pig vital signs through ground vibrations induced by heartbeat and respiration. en. In *Proceedings of the 20th ACM Conference on Embedded Networked Sensor Systems* (SenSys '22). SenSys '22: The 20th ACM Conference on Embedded Networked Sensor Systems. Association for Computing Machinery, New York,

NY, USA, (Jan. 24, 2023), 1102–1108. ISBN: 978-1-4503-9886-2. doi:10.1145/3560905.3568416.

[21] Yiwen Dong, Jonathon Fagert, and Hae Young Noh. 2023. Characterizing the variability of footstep-induced structural vibrations for open-world person identification. en. *Mechanical Systems and Signal Processing*, 204, (Dec. 2023), 110756. doi:10.1016/j.ymssp.2023.110756.

[22] Yiwen Dong, Jonathon Fagert, Pei Zhang, and Hae Young Noh. 2021. Non-parametric bayesian learning for newcomer detection using footstep-induced floor vibration: poster abstract. en. In *Proceedings of the 20th International Conference on Information Processing in Sensor Networks (Co-Located with Cps-iot Week 2021)*. IPSN '21: The 20th International Conference on Information Processing in Sensor Networks. ACM, Nashville TN USA, (May 18, 2021), 404–405. ISBN: 978-1-4503-8098-0. doi:10.1145/3412382.3458785.

[23] Yiwen Dong, Jonathon Fagert, Pei Zhang, and Hae Young Noh. 2023. Stranger detection and occupant identification using structural vibrations. en. In *European Workshop on Structural Health Monitoring*. Vol. 253. Piervincenzo Rizzo and Alberto Milazzo, (Eds.) Springer International Publishing, Cham, 905–914. ISBN: 978-3-031-07254-3. doi:10.1007/978-3-031-07254-3_91.

[24] Yiwen Dong, Megan Iammarino, Jingxiao Liu, Jesse Codling, Jonathon Fagert, Mostafa Mirshekari, Linda Lowes, Pei Zhang, and Hae Young Noh. 2024. Ambient floor vibration sensing advances the accessibility of functional gait assessments for children with muscular dystrophies. en. *Scientific Reports*, 14, 1, (May 11, 2024), 10774. doi:10.1038/s41598-024-60034-5.

[25] Yiwen Dong, Sung Eun Kim, Kornél Schadl, Peide Huang, Wenhao Ding, Jessica Rose, and Hae Young Noh. 2024. In-home gait abnormality detection through footstep-induced floor vibration sensing and person-invariant contrastive learning. en. *IEEE Journal of Biomedical and Health Informatics*, 28, 12, (Dec. 2024), 7054–7067. doi:10.1109/JBHI.2024.3413815.

[26] Yiwen Dong, Jingxiao Liu, Sung Eun Kim, Kornél Schadl, Jessica Rose, and Hae Young Noh. 2025. Graphical modeling of the lower-limb joint motion from the dynamic floor responses under footstep forces. en. In *Dynamics of Civil Structures, Vol. 2*. Matthew Whelan, P. Scott Harvey, and Fernando Moreu, (Eds.) Springer Nature Switzerland, Cham, 9–16. ISBN: 978-3-031-68889-8. doi:10.1007/978-3-031-68889-8_2.

[27] Yiwen Dong, Jingxiao Liu, and Hae Young Noh. 2022. GaitVibe+: enhancing structural vibration-based footstep localization using temporary cameras for in-home gait analysis. en. In *Proceedings of the 20th ACM Conference on Embedded Networked Sensor Systems*. SenSys '22: The 20th ACM Conference on Embedded Networked Sensor Systems. ACM, Boston Massachusetts, (Nov. 6, 2022), 1168–1174. ISBN: 978-1-4503-9886-2. doi:10.1145/3560905.3568435.

[28] Yiwen Dong and Hae Young Noh. 2024. Human gait parameter and health information extraction using floor-mounted geophone sensors. en. (Dec. 26, 2024). U.S. pat. Patent No. 20240423503A1. Leland Stanford Junior University. Retrieved Feb. 13, 2025 from https://patents.google.com/patent/US20240423503A1/en?oq=US20240423503.

[29] Yiwen Dong and Hae Young Noh. 2024. Structure-agnostic gait cycle segmentation for in-home gait health monitoring through footstep-induced structural vibrations. en. In *Dynamics of Civil Structures, Volume 2*. Hae Young Noh, Matthew Whelan, and P. Scott Harvey, (Eds.) Springer Nature Switzerland, Cham, 65–74. ISBN: 978-3-031-36662-8. doi:10.1007/978-3-031-36663-5_8.

[30] Yiwen Dong and Hae Young Noh. 2024. Ubiquitous gait analysis through footstep-induced floor vibrations. en. *Sensors*, 24, 8, (Apr. 13, 2024), 2496. doi:10.3390/s24082496.

[31] Yiwen Dong, Zihao Song, Jesse Codling, Gary Rohrer, Jeremy Miles, Raj Sharma, Tami Brown-Brandl, Pei Zhang, and Hae Young Noh. 2024. Robust piglet nursing behavior monitoring through multi-modal fusion of computer vision and ambient floor vibration. en. (Oct. 15, 2024). Social Science Research Network: 4987438. Pre-published.

[32] Yiwen Dong, Haochen Sun, Ruizhi Wang, and Hae Young Noh. 2024. Robust personalized gait health monitoring through footstep-induced structural vibrations. en. In *Sensors and Smart Structures Technologies for Civil, Mechanical, and Aerospace Systems 2024*. Sensors and Smart Structures Technologies for Civil, Mechanical, and Aerospace Systems 2024. Maria Pina Limongelli, Ching Tai Ng, and Branko Glisic, (Eds.) SPIE, Long Beach, United States, (May 9, 2024), 49. ISBN: 978-1-5106-7204-8. doi:10.1117/12.3010554.

[33] Yiwen Dong, Yuyan Wu, Yen-Cheng Chang, Jatin Aggarwal, Jesse R. Codling, Hugo Latapie, Pei Zhang, and Hae Young Noh. 2024. Context-aware crowd monitoring for sports games using crowd-induced floor vibrations. en. *Data-Centric Engineering*, 5, (Jan. 2024), e25. doi:10.1017/dce.2024.28.

[34] Yiwen Dong, Yuyan Wu, Jesse R Codling, Jatin Aggarwal, Peide Huang, Wenhao Ding, Hugo Latapie, Pei Zhang, and Hae Young Noh. 2023. GameVibes: vibration-based crowd monitoring for sports games through audience-game-facility association modeling. en. In *Proceedings of the 10th ACM International Conference on Systems for Energy-efficient Buildings, Cities, and Transportation* (BuildSys '23). BuildSys '23: The 10th ACM International Conference on Systems for Energy-Efficient Buildings, Cities, and Transportation. Association for Computing Machinery, Istanbul Turkey, (Nov. 15, 2023), 177–188. ISBN: 979-8-4007-0230-3. doi:10.1145/3600100.3623750.

[35] Yiwen Dong, Yuyan Wu, Sung Eun Kim, Kornél Schadl, Jessica Rose, and Hae Young Noh. 2025. Modeling foot–floor interactions during walking for normal and abnormal gaits. en. *Journal of Engineering Mechanics*, 151, 1, (Jan. 1, 2025), 4024100. doi:10.1061/JENMDT.EMENG-7639.

[36] Yiwen Dong, Yuyan Wu, and Hae Young Noh. 2023. Detecting gait abnormalities in foot-floor contacts during walking through footstep-induced structural vibrations. en. In *Proceedings of the 14th International Workshop on Structural Health Monitoring*. Structural Health Monitoring 2023. Destech Publications, Inc., (Sept. 12, 2023). ISBN: 978-1-60595-693-0. arXiv: 2405.13996 [eess]. doi:10.12783/shm2023/36965.

[37] Yiwen Dong, Jiacheng Zhu, and Hae Young Noh. 2022. Re-vibe: vibration-based indoor person re-identification through cross-structure optimal transport. en. In *Proceedings of the 9th ACM International Conference on Systems for Energy-efficient Buildings, Cities, and Transportation*. BuildSys '22: The 9th ACM International Conference on Systems for Energy-Efficient Buildings, Cities, and Transportation. ACM, Boston Massachusetts, (Nov. 9, 2022), 348–352. ISBN: 978-1-4503-9890-9. doi:10.1145/3563357.3566134.

[38] Yiwen Dong, Joanna Jiaqi Zou, Jingxiao Liu, Jonathon Fagert, Mostafa Mirshekari, Linda Lowes, Megan Iammarino, Pei Zhang, and Hae Young Noh. 2020. MD-vibe: physics-informed analysis of patient-induced structural vibration data for monitoring gait health in individuals with muscular dystrophy. en. In *Adjunct Proceedings of the 2020 ACM International Joint Conference on Pervasive and Ubiquitous Computing and Proceedings of the 2020 ACM International Symposium on Wearable Computers*. UbiComp/ISWC '20: 2020 ACM International Joint Conference on Pervasive and Ubiquitous Computing and 2020 ACM International Symposium on Wearable Computers. ACM, Virtual Event Mexico, (Sept. 10, 2020), 525–531. ISBN: 978-1-4503-8076-8. doi:10.1145/3410530.3414610.

[39] Yiwen Dong et al. 2023. PigSense: structural vibration-based activity and health monitoring system for pigs. en. *ACM Transactions on Sensor Networks*, 20, 1, (June 15, 2023), 1–43. doi:10.1145/3604806.

[40] [n. d.] ESP8266 wi-fi SoC | espressif systems. en. Retrieved July 3, 2025 from https://www.espressif.com/en/products/socs/esp8266.

[41] Jonathon Fagert, Amelie Bonde, Sruti Srinidhi, Sarah Hamilton, Pei Zhang, and Hae Young Noh. 2022. Clean vibes: hand washing monitoring using structural vibration sensing. en. *ACM Trans. Comput. Healthcare*, 3, 3, (July 5, 2022), 34:1–34:25. doi:10.1145/3511890.

[42] Jonathon Fagert, Mostafa Mirshekari, Shijia Pan, Linda Lowes, Megan Iammarino, Pei Zhang, and Hae Young Noh. 2021. Structure-and sampling-adaptive gait balance symmetry estimation using footstep-induced structural floor vibrations. en. *Journal of Engineering Mechanics*, 147, 2, 4020151. doi:10.1061/(ASCE)EM.1943-7889.0001889.

[43] Jonathon Fagert, Mostafa Mirshekari, Shijia Pan, Pei Zhang, and Hae Young Noh. 2017. Characterizing left-right gait balance using footstep-induced structural vibrations. en. In *Sensors and Smart Structures Technologies for Civil, Mechanical, and Aerospace Systems 2017*. Sensors and Smart Structures Technologies for Civil, Mechanical, and Aerospace Systems 2017. Vol. 10168. SPIE, Portland, Oregon, United States, (Apr. 12, 2017), 357–365. doi:10.1117/12.2260376.

[44] Jonathon Fagert, Mostafa Mirshekari, Shijia Pan, Pei Zhang, and Hae Young Noh. 2019. Characterizing structural changes to estimate walking gait balance. en. In *Dynamics of Civil Structures, Volume 2*. Springer, 333–335.

[45] Jonathon Fagert, Mostafa Mirshekari, Shijia Pan, Pei Zhang, and Hae Young Noh. 2019. Vibration source separation for multiple people gait monitoring using footstep-induced floor vibrations. en. In *Structural Health Monitoring 2019*. Structural Health Monitoring 2019. DEStech Publications, Inc., (Nov. 15, 2019). ISBN: 978-1-60595-601-5. doi:10.12783/shm2019/32338.

[46] Jonathon Fagert, Mostafa Mirshekari, Shijia Pan, Pei Zhang, and Hae Young Noh. 2017. Monitoring hand-washing practices using structural vibrations. en. In *Structural Health Monitoring 2017*. Structural Health Monitoring 2017. DEStech Publications, Inc., (Sept. 28, 2017). ISBN: 978-1-60595-330-4. doi:10.12783/shm2017/14133.

[47] A. Garrigós, D. Marroquí, J. M. Blanes, R. Gutiérrez, I. Blanquer, and M. Cantó. 2017. Designing arduino electronic shields: experiences from secondary and university courses. en. In *2017 IEEE Global Engineering Education Conference (EDUCON)*. 2017 IEEE Global Engineering Education Conference (EDUCON). IEEE, Athens, Greece, (Apr. 2017), 934–937. ISBN: 978-1-5090-5467-1. doi:10.1109/EDUCON.2017.7942960.

[48] Madhumitha Harishankar et al. 2020. LaNet: real-time lane identification by learning road SurfaceCharacteristics from accelerometer data. en. (Apr. 6, 2020). arXiv: 2004.02822 [cs]. Pre-published.

[49] Kaiming He, Xiangyu Zhang, Shaoqing Ren, and Jian Sun. 2016. Deep residual learning for image recognition. en. In *2016 IEEE Conference on Computer Vision and Pattern Recognition (CVPR)*. 2016 IEEE Conference on Computer Vision and Pattern Recognition (CVPR). IEEE, Las Vegas, NV, USA, (June 2016), 770–778. ISBN: 978-1-4673-8851-1. doi:10.1109/CVPR.2016.90.

[50] G. M. Hoover and J. T. O'Brien. 1980. The influence of the planted geophone on seismic land data. en. *Geophysics*, 45, 8, (Aug. 1980), 1239–1253. doi:10.1190/1.1441121.

[51] Zhizhang Hu, Emre Sezgin, Simon Lin, Pei Zhang, Hae Young Noh, and Shijia Pan. 2019. Device-free sleep stage recognition through bed frame vibration sensing. en. In *Proceedings of the 1st ACM International Workshop on Device-free Human Sensing* (DFHS'19). BuildSys '19: The 6th ACM International Conference on Systems for Energy-Efficient Buildings, Cities, and Transportation. Association for Computing Machinery, New York, NY, USA, (Nov. 10, 2019), 39–43. ISBN: 978-1-4503-7007-3. doi:10.1145/3360773.3360883.

[52] 2020. IEEE standard for a precision clock synchronization protocol for networked measurement and control systems. en. *IEEE Std 1588-2019 (revision Ofieee Std 1588-2008)*, (June 2020), 1–499. doi:10.1109/IEEESTD.2020.9120376.

[53] 2025. IEEE standard for information technology–telecommunications and information exchange between systems local and metropolitan area networks–specific requirements part 11: wireless LAN medium access control (MAC) and physical layer (PHY) specifications. en. *IEEE Std 802.11-2024 (revision of IEEE Std 802.11-2020)*, (Apr. 2025), 1–5956. doi:10.1109/IEEESTD.2025.10979691.

[54] 2020. IEEE standard for low-rate wireless networks. en. *IEEE Std 802.15.4-2020 (revision of IEEE Std 802.15.4-2015)*, (July 2020), 1–800. doi:10.1109/IEEESTD.2020.9144691.

[55] [n. d.] IP65 NEMA 4X box PN-1323. en. Bud Industries. Retrieved June 3, 2025 from https://www.budind.com/series/nema-ip-rated-boxes/pn-series-nema-box/.

[56] [SW], KiCad EDA 1992. URL: https://kicad.org.

[57] Jin-Shyan Lee, Yu-Wei Su, and Chung-Chou Shen. 2007. A comparative study of wireless protocols: bluetooth, UWB, ZigBee, and wi-fi. en. In *IECON 2007 - 33rd Annual Conference of the IEEE Industrial Electronics Society*. IECON 2007 - 33rd Annual Conference of the IEEE Industrial Electronics Society. IEEE, Taipei, Taiwan, (Nov. 2007), 46–51. ISBN: 978-1-4244-0783-5. doi:10.1109/IECON.2007.4460126.

[58] [SW] Roger A. Light, Mosquitto: Server and Client Implementation of the MQTT Protocol version 2.0.21, 2017. Eclipse Foundation. doi:10.21105/joss.00265.

[59] Jingxiao Liu, Bingqing Chen, Siheng Chen, Mario Berges, Jacobo Bielak, and HaeYoung Noh. 2020. Damage-sensitive and domain-invariant feature extraction for vehicle-vibration-based bridge health monitoring. en. In *ICASSP 2020 - 2020 IEEE International Conference on Acoustics, Speech and Signal Processing (ICASSP)*. ICASSP 2020 - 2020 IEEE International Conference on Acoustics, Speech and Signal Processing (ICASSP). IEEE, Barcelona, Spain, (May 2020), 3007–3011. ISBN: 978-1-5090-6631-5. doi:10.1109/ICASSP40776.2020.9053450.

[60] Jingxiao Liu, Siyuan Yuan, Yiwen Dong, Biondo Biondi, and Hae Young Noh. 2023. TelecomTM: a fine-grained and ubiquitous traffic monitoring system using pre-existing telecommunication fiber-optic cables as sensors. en. *Proceedings of the ACM on Interactive, Mobile, Wearable and Ubiquitous Technologies*, 7, 2, (June 12, 2023), 1–24. doi:10.1145/3596262.

[61] Rohan Menon, Rohit Gujarathi, Ali Saffari, and Joshua R. Smith. 2022. Wireless identification and sensing platform version 6.0. en. In *Proceedings of the 20th ACM Conference on Embedded Networked Sensor Systems*. SenSys '22: The 20th ACM Conference on Embedded Networked Sensor Systems. ACM, Boston Massachusetts, (Nov. 6, 2022), 899–905. ISBN: 978-1-4503-9886-2. doi:10.1145/3560905.3568109.

[62] Mostafa Mirshekari, Jonathon Fagert, Amelie Bonde, Pei Zhang, and Hae Young Noh. 2018. Human gait monitoring using footstep-induced floor vibrations across different structures. en. In *Proceedings of the 2018 ACM International Joint Conference and 2018 International Symposium on Pervasive and Ubiquitous Computing and Wearable Computers* (UbiComp '18). UbiComp '18: The 2018 ACM International Joint Conference on Pervasive and Ubiquitous Computing. Association for Computing Machinery, New York, NY, USA, (Oct. 8, 2018), 1382–1391. ISBN: 978-1-4503-5966-5. doi:10.1145/3267305.3274187.

[63] Mostafa Mirshekari, Jonathon Fagert, Shijia Pan, Pei Zhang, and Hae Young Noh. 2019. Physics-guided model transfer for human gait monitoring using footstep-induced floor vibration. en. In *Structural Health Monitoring 2019*. Structural Health Monitoring 2019. DEStech Publications, Inc., (Nov. 15, 2019). ISBN: 978-1-60595-601-5. doi:10.12783/shm2019/32337.

[64] Mostafa Mirshekari, Jonathon Fagert, Shijia Pan, Pei Zhang, and Hae Young Noh. 2020. Step-level occupant detection across different structures through footstep-induced floor vibration using model transfer. en. *Journal of Engineering Mechanics*, 146, 3, (Mar. 1, 2020), 4019137, 3, (Mar. 1, 2020). doi:10.1061/(ASCE)EM.1943-7889.0001719.

[65] Frank Mokaya, Roland Lucas, Hae Young Noh, and Pei Zhang. 2016. Burnout: a wearable system for unobtrusive skeletal muscle fatigue estimation. en. In *2016 15th ACM/IEEE International Conference on Information Processing in Sensor Networks (IPSN)*. 2016 15th ACM/IEEE International Conference on Information Processing in Sensor Networks (IPSN). IEEE, Vienna, Austria, (Apr. 2016), 1–12. ISBN: 978-1-5090-0802-5. doi:10.1109/IPSN.2016.7460661.

[66] Shijia Pan, Mario Berges, Juleen Rodakowski, Pei Zhang, and Hae Young Noh. 2019. Fine-grained recognition of activities of daily living through structural vibration and electrical sensing. en. In *Proceedings of the 6th ACM International Conference on Systems for Energy-efficient Buildings, Cities, and Transportation*. BuildSys '19: The 6th ACM International Conference on Systems for Energy-Efficient Buildings, Cities, and Transportation. ACM, New York NY USA, (Nov. 13, 2019), 149–158. ISBN: 978-1-4503-7005-9. doi:10.1145/3360322.3360851.

[67] Shijia Pan, Amelie Bonde, Jie Jing, Lin Zhang, Pei Zhang, and Hae Young Noh. 2014. BOES: building occupancy estimation system using sparse ambient vibration monitoring. en. In *Sensors and Smart Structures Technologies for Civil, Mechanical, and Aerospace Systems 2014*. Sensors and Smart Structures Technologies for Civil, Mechanical, and Aerospace Systems 2014. Vol. 9061. International Society for Optics and Photonics, San Diego, California, USA, (Apr. 10, 2014), 90611O. doi:10.1117/12.2046510.

[68] Shijia Pan, Mostafa Mirshekari, Jonathon Fagert, Ceferino Gabriel Ramirez, Albert Jin Chung, Chih Chi Hu, John Paul Shen, Pei Zhang, and Hae Young Noh. 2018. Characterizing human activity induced impulse and slip-pulse excitations through structural vibration. en. *Journal of Sound and Vibration*, 414, (Feb. 3, 2018), 61–80. doi:10.1016/j.jsv.2017.10.034.

[69] Shijia Pan, Susu Xu, Mostafa Mirshekari, Pei Zhang, and Hae Young Noh. 2017. Collaboratively adaptive vibration sensing system for high-fidelity monitoring of structural responses induced by pedestrians. en. *Frontiers in Built Environment*, 3, 28. doi:10.3389/fbuil.2017.00028.

[70] Shijia Pan, Tong Yu, Mostafa Mirshekari, Jonathon Fagert, Amelie Bonde, Ole J. Mengshoel, Hae Young Noh, and Pei Zhang. 2017. FootprintID: indoor pedestrian identification through ambient structural vibration sensing. en. *Proceedings of the ACM on Interactive, Mobile, Wearable and Ubiquitous Technologies*, 1, 3, (Sept. 11, 2017), 1–31, 3, (Sept. 11, 2017). doi:10.1145/3130954.

[71] E. Dalila Pinedo-Frausto and J. Antonio Garcia-Macias. 2008. An experimental analysis of zigbee networks. en. In *2008 33rd IEEE Conference on Local Computer Networks (LCN)*. 2008 33rd IEEE Conference on Local Computer Networks (LCN). IEEE, Montreal, QB, Canada, (Oct. 2008), 723–729. ISBN: 978-1-4244-2412-2. doi:10.1109/LCN.2008.4664272.

[72] [SW], PlatformIO: Your Gateway to Embedded Software Development Excellence 2014. URL: https://platformio.org.

[73] Joseph Polastre, Robert Szewczyk, and David Culler. 2005. Telos: enabling ultra-low power wireless research. en. In *Proceedings of the 4th International Symposium on Information Processing in Sensor Networks* (IPSN '05). IEEE Press, Los Angeles, California, (Apr. 24, 2005), 48–es. ISBN: 978-0-7803-9202-1. doi:10.5555/1147685.

[74] 2020. SM-24 equivalent geophone sensor | high precision sensor. en. (July 8, 2020). Retrieved June 22, 2024 from https://www.seis-tech.com/sm-24-equivalent-geophone-sensor/.

[75] [SW], Sparkfun/OpAmp_breakout-LMV358 version 1.6, Sept. 16, 2021. SparkFun Electronics. URL: https://github.com/sparkfun/OpAmp_Breakout-LMV358Retrieved July 3, 2025 from.

[76] Yuyan Wu, Yiwen Dong, Sumer Vaid, Gabriella M. Harari, and Hae Young Noh. 2023. Emotion recognition using footstep-induced floor vibration signals. en. In *Proceedings of the 14th International Workshop on Structural Health Monitoring*. Structural Health Monitoring 2023. Destech Publications, Inc., (Sept. 12, 2023). ISBN: 978-1-60595-693-0. doi:10.12783/shm2023/36968.

[77] Duli Yu, Darron Collins, and Bernard Maechler. 2009. MEMS accelerometer vs. geophone for seismic monitoring and survey. en. In *Beijing 2009 International Geophysical Conference and Exposition, Beijing, China, 24?27 April 2009*. SEG Global Meeting Abstracts. Society of Exploration Geophysicists, Beijing, China, (Apr. 24, 2009), 9–9. ISBN: 978-1-56080-284-6. doi:10.1190/1.3603534.

[78] Yue Zhang, Zhizhang Hu, Uri Berger, and Shijia Pan. 2023. CMA: cross-modal association between wearable and structural vibration signal segments for indoor occupant sensing. en. In *The 22nd International Conference on Information Processing in Sensor Networks*. IPSN '23: The 22nd International Conference on Information Processing in Sensor Networks. ACM, San Antonio TX USA, (May 9, 2023), 96–109. ISBN: 979-8-4007-0118-4. doi:10.1145/3583120.3586960.

[79] Yue Zhang, Shijia Pan, Jonathon Fagert, Mostafa Mirshekari, Hae Young Noh, Pei Zhang, and Lin Zhang. 2018. Vibration-based occupant activity level monitoring system. en. In *Proceedings of the 16th ACM Conference on Embedded Networked Sensor Systems*. SenSys '18: The 16th ACM Conference on Embedded Networked Sensor Systems. ACM, Shenzhen China, (Nov. 4, 2018), 349–350. ISBN: 978-1-4503-5952-8. doi:10.1145/3274783.3275177.